A flexible agent-based modelling framework of multi-serotype pneumococcal carriage to evaluate vaccine strategies in large populations

Nefel Tellioglu[1], David Price[1], Xinghui Chen[1], Violeta Spirkoska[1], Yingying Wang[2], Robert Moss[2], Natalie Carvalho[2], Kylie Carville[1], Particia T. Campbell[1], Jodie McVernon[1]

[1]University of Melbourne, Department of Infectious Diseases, Melbourne Medical School, Parkville, Australia

[2]University of Melbourne, Melbourne School of Population and Global Health, Parkville, Australia

Abstract

Streptococcus pneumoniae is a multi-serotype pathogen causing a substantial global burden of pneumonia and invasive bacterial disease. Pneumococcal conjugate vaccines have been implemented worldwide, protecting against colonisation and disease with selected high-burden serotypes, but in many settings, short-term effectiveness has been eroded by serotype replacement. Vaccines with broader serotype coverage have been developed, at the cost of immunogenicity against single serotypes. To determine the longer-term impact of these new formulations, we propose a novel modelling framework that evaluates the relationship between serotype-specific vaccine immunogenicity and effectiveness, comprising immunity, carriage and clinical models. Dynamics of individual serotypes are modelled over time, advancing existing paradigms that group all serotypes according to vaccine type. This framework is sufficiently flexible to consider diverse populations and vaccine implementation strategies. A retrospective analysis of sequential introduction of 7- and 13-valent pneumococcal conjugate vaccines in Australia validates and demonstrates the model.

1. Introduction

Streptococcus pneumoniae (S. pneumoniae) colonises the nasopharynx, but can also cause infection and both non-invasive disease, such as otitis media and pneumonia, or invasive pneumococcal disease (IPD), including meningitis and bacteraemia (*1*, *2*). Pathogenicity is largely, though not solely, determined by the polysaccharide capsular antigen (serotype) (*1*, *2*). Over 100 pneumococcal serotypes have been identified, with varying prevalence by age and geographic location (*2*, *3*). Immunogenicity characteristics, such as immunoglobulin G (IgG) concentration required for protection and potential to cause invasive disease, also vary by serotype (*2*, *4*, *5*). The substantial global burden of morbidity and mortality caused by pneumococcus is predominantly borne in low- and middle-income countries, and disproportionately affects children (*6*, *7*). Older adults and children under 5 are also at risk in high-income settings (*8*, *9*).

The notable burden of disease has driven development of several pneumococcal vaccines over time, administered according to different vaccine schedules (*3*, *5*, *10*). The first vaccines to be developed comprising polysaccharide capsular antigens were poorly immunogenic in children aged <2 years (*11*, *12*). Moreover, pneumococcal polysaccharide vaccines (PPVs) only activate the humoral arm of the immune system and fail to induce immune memory (*10*, *13*). Consequently, while PPVs provide protection against IPD, they show limited and variable efficacy in preventing community acquired pneumonia (CAP) and do not reduce nasopharyngeal colonisation, thereby failing to interrupt transmission (*14*). These limitations were overcome by the development of pneumococcal conjugate vaccines (PCVs), in which polysaccharides are conjugated to a carrier protein (*10*, *13*). Conjugation enhances immunogenicity and effectiveness by inducing immune memory, including in young children (*10*). Conjugate vaccines protect against both systemic and mucosal infection and prevent nasopharyngeal colonisation by vaccine serotypes, thereby reducing transmission in the community (*15*, *16*). A seven valent conjugate vaccine (7vPCV), first licensed in the USA in 2000, included seven serotypes causing at least 70% of disease in young children in western industrialised countries (*2*, *15*). However, serotype replacement and continuing burden of disease, has driven the creation of higher valency vaccines (*7*, *10*, *15*, *16*). A 13vPCV became available in 2010, and more recently 15vPCV, 20vPCV, and 21vPCV have been developed (*4*, *10*, *15*). However, there is some concern regarding declining immunogenicity against shared serotypes with higher-valency PCVs, with uncertain implications for effectiveness (*15*).

Variability in serotype-specific immunogenic response of multiple vaccine products necessitates a flexible approach to modelling potential impacts of different vaccines. While previous models examining use of pneumococcal vaccines account for the multi-serotype nature of *S. pneumoniae* to some degree, they often depend on simplifying assumptions about serotype (vaccine-type groupings, or inclusion of a limited number of serotypes), co-infections (no co-infections among vaccine-type groupings), immune response (homogeneous immune response to vaccine-type serotypes), and host representation (only considering a specific age group) (*17–26*). Models that group

serotypes into vaccine and non-vaccine types typically assume that there would be no co-infection with serotypes from the same group, which does not allow co-infection with two non-vaccine serotypes, for example in De Cao et al. (2014) (*18*). This assumption has the potential to alter transmission rates once vaccine-type serotype circulation decreases following vaccine introduction. Additionally, these models often assume a homogeneous vaccine-induced immune response to vaccine-type serotypes, for example in Megiddo et al. (2018) (*23*) . which does not allow observed differences in serotype-specific immunogenicity to be incorporated. These assumptions make it challenging to fully explore the effectiveness of vaccine programs, and the impact of reduced immunogenicity of higher valency vaccines on pneumococcal disease.

We have developed a flexible individual-level modelling framework that incorporates differences in vaccine immunogenicity against individual serotypes allowing estimation of relative correlates of protection from historical data. We demonstrate the value of this model framework by considering the introduction of 7vPCV and 13vPCV in Australia in recent decades. The validated model can be used to anticipate the likely impact of future expanded valency vaccines with diverse serotype composition.

2. Methods

Our modelling framework is comprised of three integrated models (Fig 1):

1. **An immunity model**: of immune responses within individuals, incorporating available evidence on age-specific initial levels of vaccine-induced antibody titres and waning dynamics of immune responses,
2. **A transmission model**: capturing transmission amongst the population of multiple serotypes of pneumococcal infection (carriage),
3. **A clinical model**: representing the progression of infection to clinical outcomes of importance, namely IPD and CAP, according to serotype. The clinical model incorporates available evidence on age-specific IPD and CAP outcome rates.

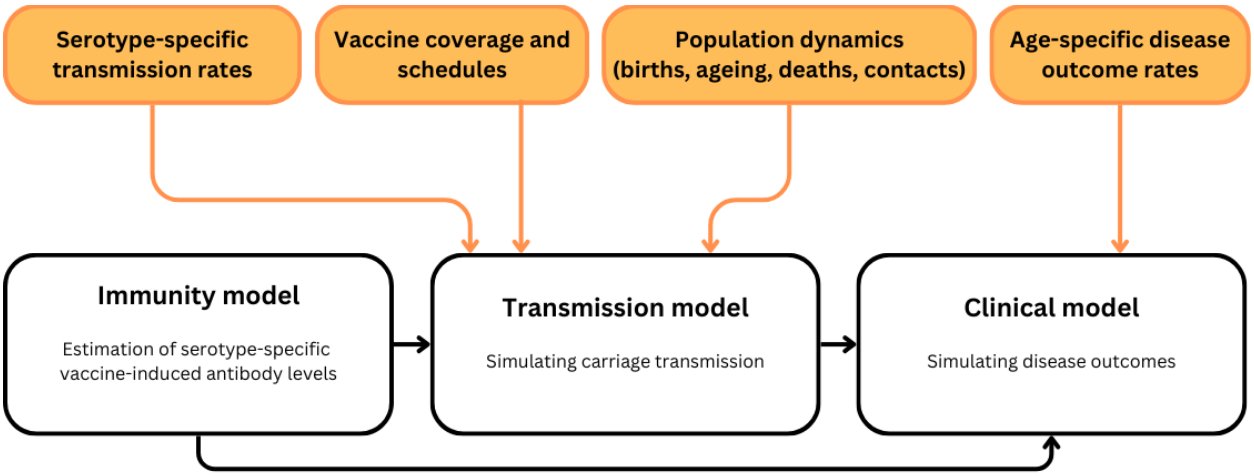

Fig 1: Modelling procedure diagram

In the following, we provide a detailed explanation of the immunity, transmission, and clinical models, the model calibration and the scenarios we consider for our subsequent analyses.

2.1. Immunity model

An individual's initial vaccine-induced antibody response to each serotype is drawn from a distribution derived from literature, and these antibodies wane over time (described below). At the time of exposure to an infected individual (determined within the transmission model), the individual's antibody level modifies their probability of being infected. If they become infected, their antibody level further informs their probability of progressing to disease (within the clinical model).

Fig 2 below provides an example of this process for a single individual.

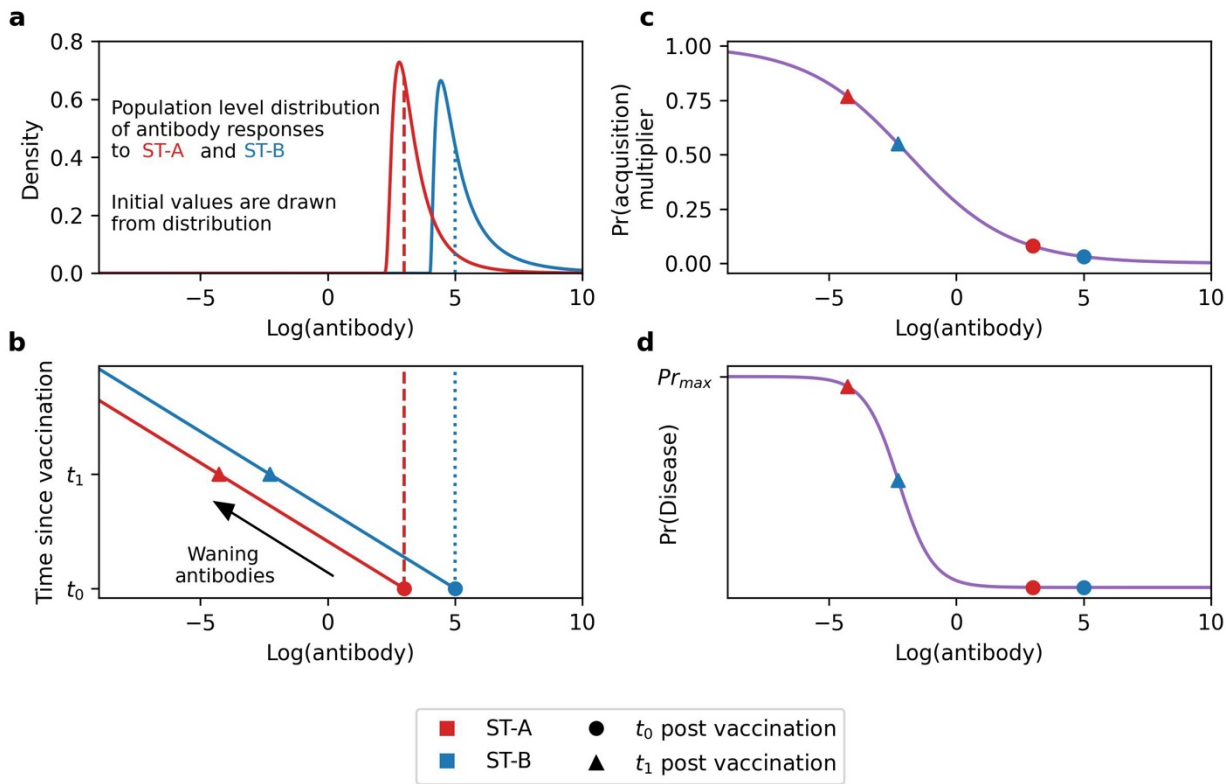

Fig 2: An exemplar implementation of vaccine-induced antibody levels for a given vaccine product and two exposed serotypes (ST-A and ST-B) in the immunity model. In this example, we assume that ST-A and ST-B are both vaccine-type serotypes. Panel a shows population level distribution of initial antibody responses to ST-A (red) and ST-B (blue). Dashed and dotted lines are the sampled initial antibody responses to ST-A (red) and ST-B (blue), respectively, for a given individual. Panel b shows the calculation of waned log-antibody titres from t_0 to t_1 post-vaccination. Panel c shows the probability of acquisition multiplier given log-antibody titres, which is used in the transmission model. Panel d shows the age-specific probability of developing IPD or CAP given an infection by serotypes ST-A and ST-B and log-antibody titres against those serotypes, which is used in the clinical model.

For the vaccinated individuals, we assume a logistic function for the vaccine-induced probability of acquisition multiplier to the serotype *a*, V_a, of the form:

$$\mathrm{V_a} = \frac{1}{1 + \mathrm{k_{acq}} * \mathrm{e}^{(\log(\mathrm{Ab})_\mathrm{a} - \mathrm{l_{acq}})}}$$

where:

- $\mathrm{k_{acq}}$ = Logistic growth rate parameter

- l_{acq} = Sigmoid midpoint
- $\log(Ab)_a$ = Vaccine-induced log-transformed (ln) antibodies to the exposed serotype *a*

For the vaccinated individuals in age group *i*, newly infected by a given serotype, *a*, we assume a similar logistic function for the probability of developing disease, of the form:

$$\Pr(\text{ Disease} \mid \text{Infection by serotype a}) = \frac{\Pr^{i}_{max}}{1 + k^{i}_{dis} * e^{(s_{dis} * (\log(Ab)_a + l^{i}_{dis}))}}$$

where:

- $\Pr^{i}_{max}$ = Maximum probability of developing disease given infection for age group *i*
- k^{i}_{dis} = Logistic growth rate parameter of age group *i*
- l^{i}_{dis} = Sigmoid midpoint of age group *i*
- s_{dis} = Scaler parameter
- $\log(Ab)_a$ = Vaccine-induced log-transformed (ln) antibodies to the exposed serotype *a*

2.1.1 Vaccine-induced Immunity Model

We conducted a rapid review of studies reporting *S. pneumoniae* antibody levels post-vaccination and revealed considerable differences in immune responses by serotype (Supplementary Material Section 1.1). We recorded antibody geometric mean concentrations (GMCs) with 95% confidence intervals for IgG from the eligible studies. We then described this heterogeneity by categorising serotypes into three groups (low, moderate, and high) according to the magnitude of the antibody responses, for each vaccine product and dose combination across multiple studies. Post-vaccination IgG antibody responses to Serotype 3 are consistently lower than to other serotypes, necessitating a separate designation (Supplementary Material Section 1.1) (*15*, *27*).

Given inconsistent/limited information on cross-reactivity of protection against serotypes that are not included in vaccine products, we assume that antibodies are generated only against serotypes in the vaccine product.

2.1.2 Naturally-acquired Immunity

Given the absence of evidence for subsequent protection against infection and disease, many pneumococcal modelling studies do not consider natural immunity following infection (*18*, *20*, *28*). Similarly, our model does not include a boost to antibodies following infection, with individuals returning to the susceptible state following clearance of

infection. We do, however, indirectly account for the accumulation of protection against pneumococcus over the life course by incorporating the observed reduction of carriage duration throughout late childhood and adult life (Supplementary Material Section 4.2).

2.2. Transmission model

The transmission model is an individual-based model that incorporates demographic and transmission dynamics. As noted in Section 2.1, we assume a susceptible-infectious-susceptible (SIS) model for *S. pneumoniae* infection, where "infection" represents carriage of *S. pneumoniae*, and disease outcomes are considered separately (in the clinical model). Similar to previous modelling studies, the infectious duration for an individual is sampled from an exponential distribution with an age-specific mean infectious duration (Table 1) (*17*, *20*, *29*, *30*). Upon recovery, infectious individuals re-enter the susceptible class, with protection derived from antibodies according to the time since their last vaccination (as dictated by the immunity model).

2.2.1 Demography

The model includes births, ageing, age-specific mortality, and age-specific migration to capture the age distribution of a population over time (Supplementary Material Section 2.1). It takes inputs of initial population size, initial age distribution, age-specific death rates, annual net birth rates, annual migration rates, and age distribution in the emigrated population to simulate demographic dynamics. We sourced the inputs from Australian Bureau of Statistics and Macro Trends Global to align with Australian population dynamics (Supplementary Material Section 4.1) (*31*, *32*) .

2.2.2 Mixing assumptions

Transmission within and between age groups is driven by contact rates, derived from synthetic contact matrices (Supplementary Material Section 2.2.1). In this work, we have assumed contacts in our population according to the contact matrices provided by Prem et al. (*33*).

2.2.3 Carriage assumptions

We assume that individuals are exposed to a single serotype at every time step. The exposed serotype is randomly selected from weighted serotype distribution in the population:

$$\Pr(\text{Exposure to serotype a}) = \frac{(\tau_a * I_a)}{\sum_s (\tau_s * I_s)}$$

where τ_a is the transmission coefficient multiplier of serotype *a*, $\mathrm{I_a}$ is the number of individuals infected by serotype *a*, and the denominator represents the sum of exposures by all the circulation serotypes, *s*. We then calculate the transmission of the exposed *S. pneumoniae* serotype for each individual. Individual infection risk for a particular serotype is determined by serotype prevalence, age, contact rates, current infection status and current antibody levels:

$$\mathrm{Pr(Infection\ by\ serotype\ a \mid exposure\ to\ serotype\ a)} = (1 - \mathrm{e}^{-\mathrm{foi_i}}) * \mathrm{V_a} * \mathrm{C}$$

where, $\mathrm{foi_i}$ represents the force of infection on an individual in age class *i*, $\mathrm{V_a}$ represents the vaccine-induced probability of acquisition multiplier to serotype *a* (see Section 2.1), and C represents the reduction of susceptibility given existing infections. We allow co-infections in the model assuming that individuals may be infected with multiple serotypes concurrently, with a reduced probability of acquiring another serotype if already infected, representing within-host competition. In this work, we assumed that C takes values of 1 (fully susceptible), 0.8 and 0 for the existing number of infections of 0, 1, and 2, respectively, which means that individuals could only be infected with two serotypes concurrently (Supplementary Material Section 2.2.4).

The force of infection comprises age-specific community transmission:

$$foi_i = q * \sum_s \tau_s * \left(\sum_j \eta_{ij} \frac{I_{js}}{N_j} \right)$$

where:

- q = Transmission coefficient
- τ_s = Transmission coefficient multiplier of serotype *s*
- η_{ij} = Number of daily community contacts between an individual in age group *i* and individuals in age group *j*
- I_{js} = Number of individuals in age group *j* infected with serotype *s*
- N_j = Number of individuals in age group *j*

This approach enables inclusion of varying transmission rates for serotypes to match the historically observed dominance of specific serotypes.

In addition to community-level circulation, we introduce serotypes externally via two processes. First, an external exposure rate simulates the ongoing introduction of serotypes through population migration, assumed to have the same age-specific and serotype-specific incidence of *S. pneumoniae* carriage as the local population (which maintains the same level of serotype and age specific carriage while population size

increases). Second, introduction of any serotype sampled uniformly from the set of all possible serotypes and therefore may not be currently circulating within the local population (which allows possibility of serotype replacement under immune selection over time).

2.2.4 Vaccination rollout programs

The model simulates the implementation of historical vaccine schedules with their rollout years, eligible age range, annual fraction of on-time and late vaccine coverages of the eligible age group, number of doses and time interval between doses. We assume that individuals receiving the first dose on time would also receive the following doses on time. We also assume that maximum protection by a vaccine starts immediately. For the simulation study, we consider vaccinations schedules shown in Table S8.

2.3. Clinical model

The clinical model takes information on the age and vaccine history of newly infected individuals from the transmission model, and the antibody levels at the time of infection, derived from these values, from the immunity model. The model then determines whether an infected individual develops a disease outcome (IPD or CAP), according to the relative probability of each occurring, and records the disease outcomes when they occur (Supplementary Material Section 3). In this work, we assume that 23vPPV is not effective against acquisition and developing CAP (*14*). In this work, the age-specific IPD to CAP ratio is calculated from the age-specific IPD and CAP incidences provided by the National Centre for Immunisation Research and Surveillance (NCIRS). IPD incidence provided by NCIRS is also available by serotype and age group.

2.4. An analysis of 13vPCV in Australia, 2002–2018

As a simulation study, we aimed to estimate the impact of the 13vPCV rollout in comparison to the continuation of 7vPCV after 2011. We compared the disease burden (CAP and IPD) across the total population in two scenarios: “With 13vPCV” (Australian vaccination strategy, 7vPCV between 2005–2010 and 13vPCV between 2011–2018) and “Without 13vPCV” (7vPCV between 2005 and 2018).

2.4.1 Data

We used historical vaccine coverage and disease rates in Australia (Supplementary Material Section 4.2). We used historical vaccine coverage from Kabir et al (2021), Frank et al (2020) and NCIRS data (Supplementary Material 4.2.2) and disease rates from NCIRS (Section 3.1) (*34*, *35*). To calculate disease rates, we used serotype and age-specific IPD cases and assumed that all J13 cases (Pneumonia due to *S. pneumoniae*), all J18.1 cases

(Lobar pneumonia) and 11% of unspecified (J15.9 and J18 except J18.1) CAP cases (using ICD-10) in Australia were caused by *S. pneumoniae* (*36*).

2.4.2 Model calibration

Disease outcomes of the model were compared with age-specific IPD and CAP rates as well as serotype proportions in IPDs between 2006–2018 provided by NCIRS. The model was initialised in 2002 with the carriage rates of the pre-vaccination era drawn from Dunne et al. (2016), and captured the overall prevalence of carriage in children aged two years and under, as well as prevalence of carriage split into 7vPCV and 13vPCV/non 7vPCV serotypes (*37*) (Table 1).

Table 1: Fixed parameters

Parameter	Description	Values	Notes/ Reference
Age-specific duration of infection (days)	Exponentially distributed with age-specific mean	0–2y: 72, 2–4y: 28, 5–17y: 18, 18+y: 17	(*17*, *20*, *29*, *30*)
Age specific probability of developing IPD when developing disease	Age specific probability of developing IPD when developing disease (IPD or CAP)	0-1m:0.314, 2-3m: 0.341, 4-5m: 0.368, 6-11m:0.279, 1-4y: 0.237, 5-14y: 0.173, 15-24y: 0.127, 25-49y: 0.136, 50-64y: 0.117, 65-74y: 0.073, 75-79y: 0.051, 80+y: 0.041	Values are estimated by age-specific IPD and CAP incidence values between 2006–2018 provided by NCIRS and population size taken from Australian Bureau of Statistics (ABS) (*31*)
Age-specific waning half-life of antibody levels (days)	-	0-17-year-olds: 125 18+-year-olds: 600	Supplementary Material Section 1
External exposure	For X times a year, Y% of the population is exposed to Z randomly selected serotypes. Individuals become infected based on the antibody levels.	X: 4, Y: 0.06, Z: 2	The values are set so that the baseline prevalence of serotypes without any vaccine introduction stays at an endemic level.
Reduction in susceptibility to co-infections (*C)*	Fractional reduction in susceptibility (between 0–1)	0.8 given one infection,	(*25*)

		1 given two infections (maximum number of co-infections is two)	
Initial number of circulating serotypes	All the serotypes in 7vPCV, 13vPCV, and 23vPPV are assumed to be circulating in the population	55	The value is set to observe at least the number of unique serotypes in Dunne et al. (2016) (*37*) and number of unique serotypes in IPD cases
Percentage of vaccine type serotypes carriage among all carriages	-	7vPCV: 55%, 13vPCV/non 7vPCV: 25%, 23vPPV/non 13vPCV: 15%, Other serotypes (NVT): 5%	(*37*)
Age-specific initial fraction of infected population	-	0–2y: 24%, 2+y: 12%	(*37*)

The percentage of IPD cases due to serotypes in each of 7vPCV, 13vPCV and 23vPPV, age-specific carriage prevalence of 7vPCV, 13vPCV/non 7vPCV, 23vPPV/non 13vPCV serotypes pre-vaccination era, and the age-specific percentage of 7vPCV, 13vPCV/non 7vPCV, 23vPPV/non 13vPCV serotypes in IPD cases between 2006–-2018 were used as summary statistics during calibration. Values of the following parameters were calibrated to match the following key trends:

Table 2: Calibrated parameters to match the observed summary statistics

Symbol(s)	Parameter(s)	Value(s)	Summary Statistics/Reference
$\boldsymbol{q}, \boldsymbol{\tau_s}$	Transmission coefficient and transmission coefficient multipliers	q : 0.0545, τ_s of 7vPCV serotypes: 1.009, τ_s of 13vPCV/non 7vPCV serotypes: 1.0063, τ_s of rest of the serotypes: 0.995	7vPCV, 13vPCV/non 7vPCV, 23vPPV/non 13vPCV carriage is set to match observed age specific prevalence (*37*)
$\boldsymbol{Pr^i_{max}}$	Maximum probability of developing disease for age group *i*	0-1m: 0.00017, 2-3m: 6.1-05, 4-5m: 7.5e-05, 6-11m: 0.0001, 1-4y: 6.0e-05, 5-14y: 1.8e-05, 15-24y: 1.3e-05, 25-49y: 3.72e-05, 50-64y: 0.00011, 65-74y: 0.00056, 75-79y: 0.0013, 80+y: 0.0028	Age-specific incidence rate of combined IPD and CAP from 2006 is used in calibration (Fig 4 and 5)

$\boldsymbol{k_{acq}}, \boldsymbol{l_{acq}}, \boldsymbol{l^i_{dis}}, \boldsymbol{k^i_{dis}}, \boldsymbol{s_{dis}}$	Probability of acquisition and probability of developing disease (sigmoid function parameters)	$k_{acq} = 5$, $l_{acq} = 1$, $l_{dis} = 1.5$, $\boldsymbol{k^i_{dis}} =$ [0-1m: 1.7, 2-3m: 2.26, 4-5m: 2.28, 6-11m: 1.57, 1-4y: 1.62, 5-14y: 6.93, 15-24y: 8.86, 25-49y: 3.83, 50-64y: 1.47, 65-74y: 0.3, 75-79y: 0.078, 80+y: 0.0015] $\boldsymbol{l^i_{dis}} =$ [0-1m: 1.91, 2-3m: 1.78, 4-5m: 1.78, 6-11m: 1.83, 1-4y: 1.78, 5-14y: 1.72, 15-24y: 1.72, 25-49y: 1.75, 50-64y: 1.84, 65-74y: 2.4, 75-79y: 3.34, 80+y: 5.23] $s_{dis} = 1.5$	Age-specific percentage of 7vPCV, 13vPCV/non 7vPCV, 23vPPV/non 13vPCV serotypes in IPD cases between 2006–2018

2.4.3 Sequential pneumococcal vaccine introduction (7vPCV, 13vPCV) in Australia, 2002–2018

In Australia, the 7vPCV paediatric (2, 4 and 6 months of age) and one dose of 23vPPV adult (65+) vaccine schedule was introduced in 2005. In 2011, the paediatric vaccine schedule was changed to 13vPCV (2, 4 and 6 months of age) with a catchup program. In the catch-up program, individuals under four years old who previously received the 7vPCV vaccine received a single dose of the 13vPCV vaccine. The 23vPPV adult vaccine rollout was maintained throughout both scenarios. The vaccine coverage data was taken from NCIRS, Kabir et al. (2021), and Frank et al. (2020) (*34*, *35*).

3. Results

3.1. Model Calibration

The modelled age-stratified incidence of IPD per year, per 100,000 over the period 2002–2018 is well aligned with data (Fig 3). The age-stratified incidence of CAP per year, per 100,000 over the period 2002–2018 is shown in Fig 4. Modelled CAP results are well aligned with the data in younger age groups. However, it is important to note that the historical *S. pneumoniae*-specific CAP cases were not available; we assumed that all cases classified as [J13 (Pneumonia due to *S. pneumoniae*) J18.1 (Lobar pneumonia)] and 11% of unspecified (J15.9 and J18 except J18.1) CAP cases using ICD-10 in Australia would be *S. pneumoniae*-specific. The proportion of vaccine-type serotypes observed in IPD cases over the period 2002–2018 is well aligned with data on IPD presentations (Fig 5).

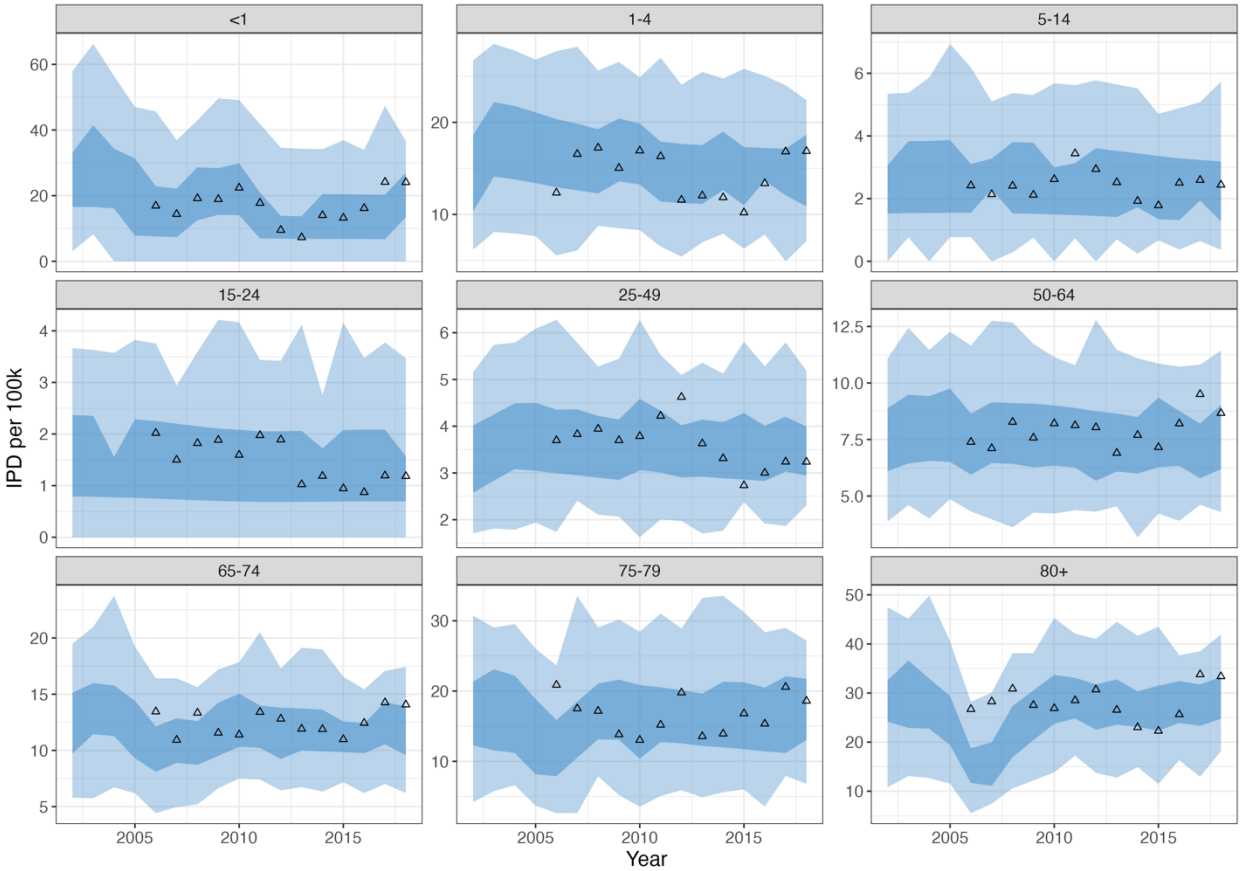

Fig 3: Age-stratified IPD incidence per year, per 100,000 for the period 2002–2018. The 50% (dark) and 95% (light) intervals of 100 simulation runs are shown as blue ribbons. Data from NCIRS is shown as triangles.

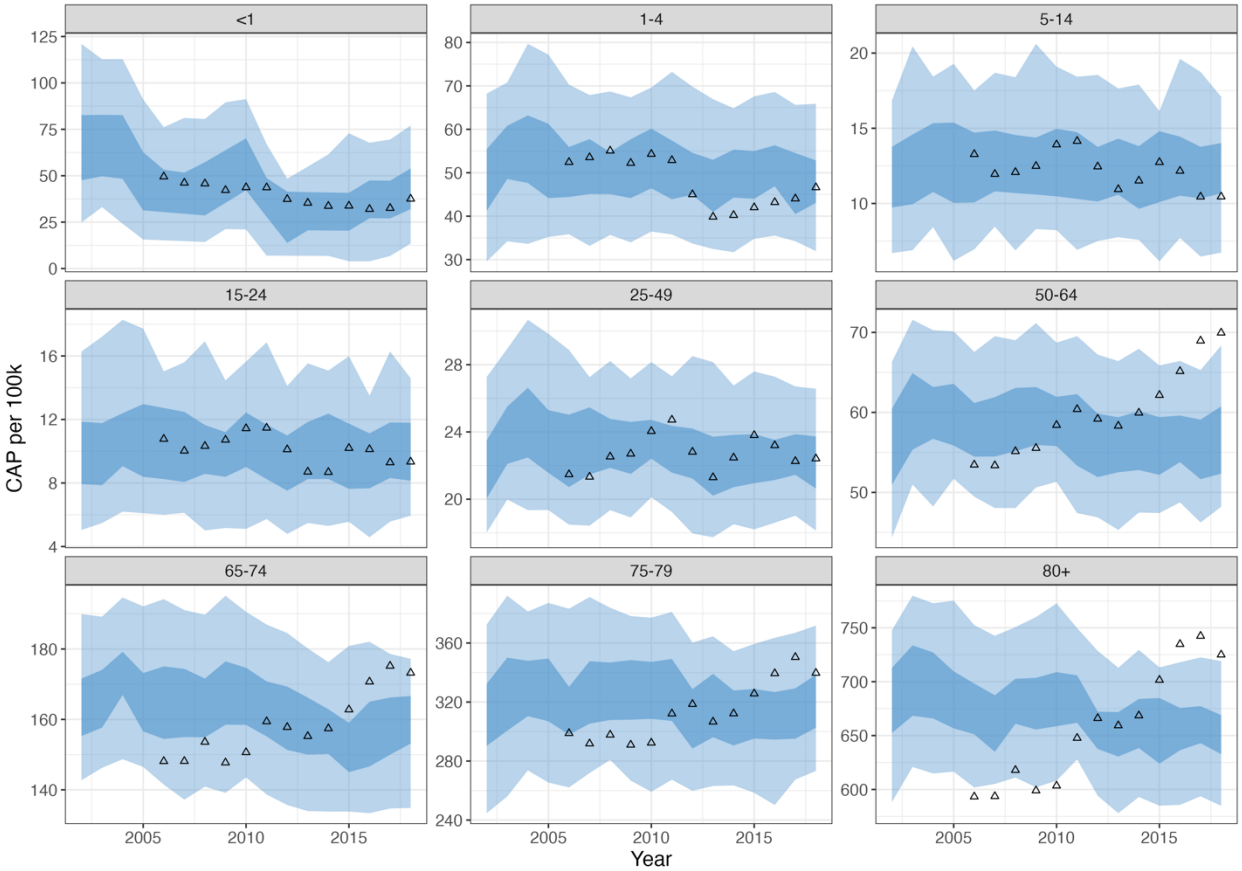

Fig 4: Age-stratified CAP incidence per year, per 100,000 for the period 2002–2018. The 50% (dark) and 95% (light) intervals of 100 simulation runs are shown as blue ribbons. Data from NCIRS is shown as triangles.

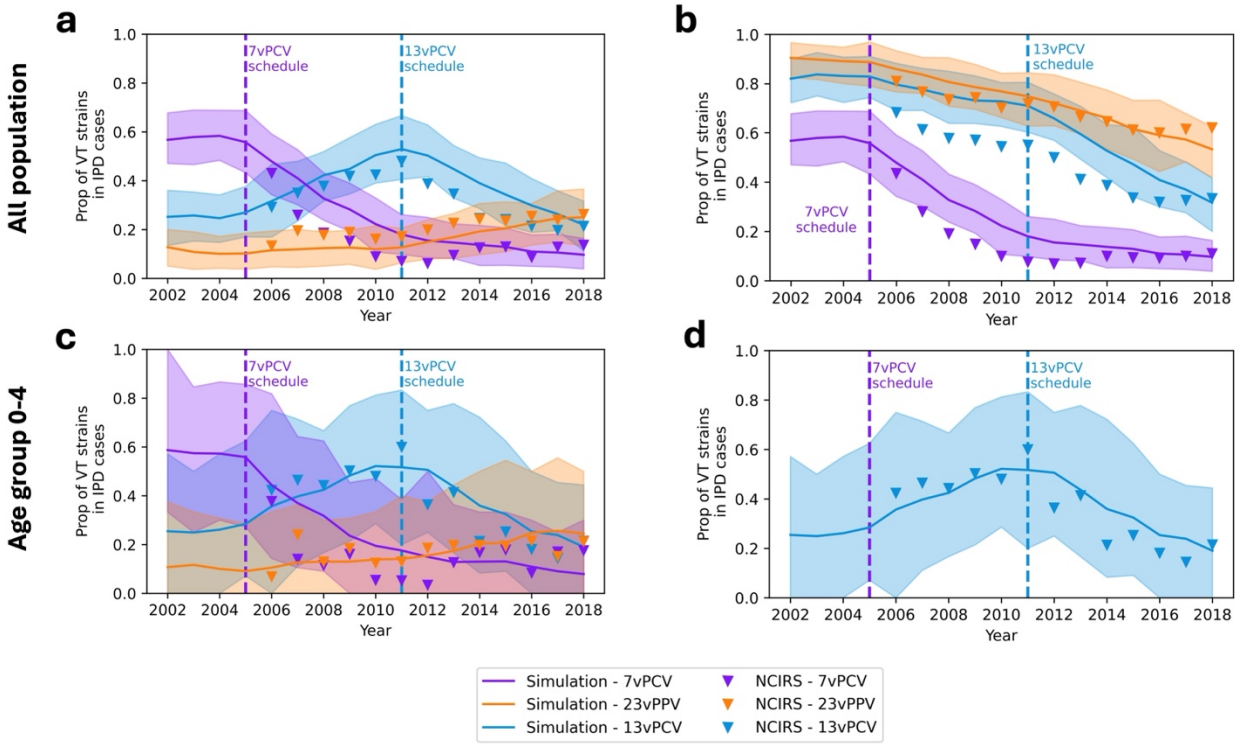

Fig 5: Proportion of vaccine-type serotypes in IPD cases for the period 2002–2018. Figures a and b report results across all population age groups, Figures c and d are restricted to IPD cases in children aged 0–4 years. Panels a and c chart the proportion of IPD cases over time attributable to 7vPCV, 13vPCV/non 7vPCV and 23vPPV/non 13vPCV vaccine-type serotypes. Panel b shows the same data as panel a, but instead of plotting serotypes specific to each vaccine, sums across all serotypes included in each of the 7vPCV, 13vPCV and 23vPPV vaccine formulations. Panel d reproduces the light blue (13vPCV/non 7vPCV) output from panel c but in isolation, for a clearer representation of trends over time. Mean and 95% quantiles of 100 simulation runs are presented, and data provided by NCIRS is shown as triangles.

3.2. The analysis of 13vPCV in Australia, 2002–2018

Modelled carriage prevalence over the period 2002–2018 separated into 7vPCV, 13vPCV and 23vPPV serotypes captures phenomenological features of serotype replacement in pneumococcal disease known to have occurred throughout this period, as demonstrated by shifts in the proportion of vaccine type serotypes in IPD cases (Fig 6a). At the start of the funded vaccination program in 2005, modelled carriage prevalence of the serotypes in 7vPCV begins to decrease, while the non-vaccine types (NVT) at that time (i.e., 13vPCV/non 7vPCV, 23vPPV/non 13vPCV and NVT) all rise. In 2011, when 13vPCV was introduced, prevalence of included serotypes similarly decreases, while 23vPPV/non

13vPCV and NVT continue to increase. In the no 13vPCV scenario, we observe a continued increase in the carriage of 13vPCV serotypes and a decrease of 23vPPV/non 13vPCV serotypes (Fig 6b).

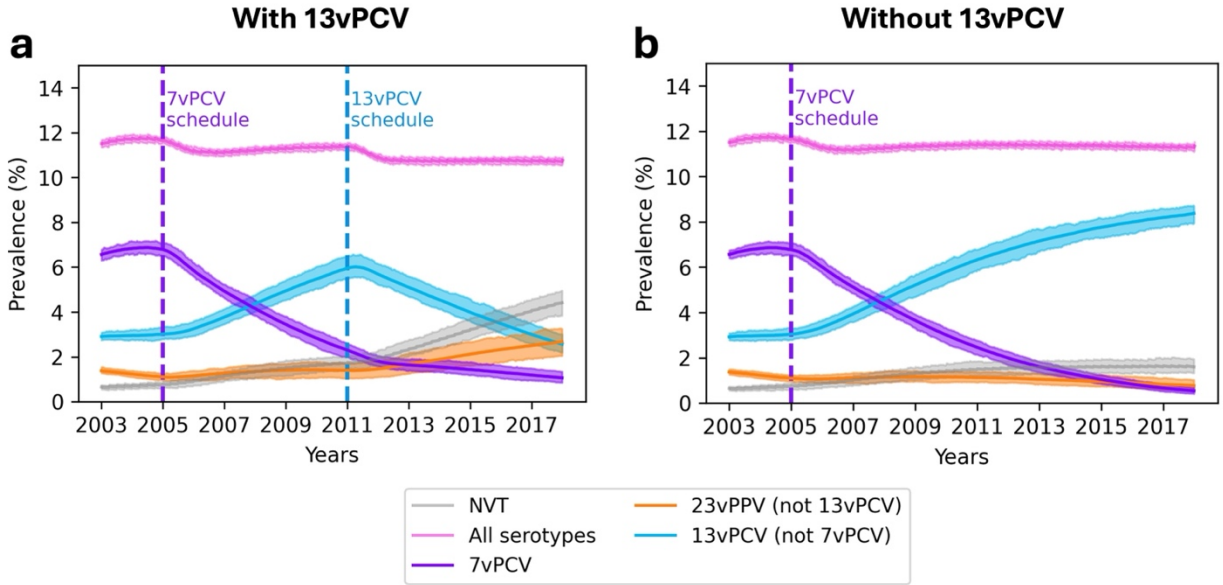

Fig 6: Prevalence of serotypes from 2002–2018, grouped into 7vPCV, 13vPCV/non 7vPCV, 23vPPV/non 13vPCV. The results of 100 simulation runs are presented in each panel, with lines representing the mean for each serotype (shading represents 95% quantiles).

In the absence of 13vPCV, our model suggests we would have observed a further decline in the proportion of 7vPCV serotypes in IPD cases per year, per 100,000 after 2012 (Fig. 7). Due to the higher transmissibility of 13vPCV serotypes compared to non-13vPCV serotypes, the carriage of 23vPPV/non13vPCV serotypes decreased over time due to competition (Fig. 6.b). This led to fewer IPD cases per year, per 100,000 from 23vPPV/non 13vPCV serotypes and an increase in cases from serotype 6A (the only 13vPCV/non 23vPPV serotype), resulting in more IPD cases from 13vPCV serotypes than from 23vPPV serotypes after 2012 (Fig 7.b).

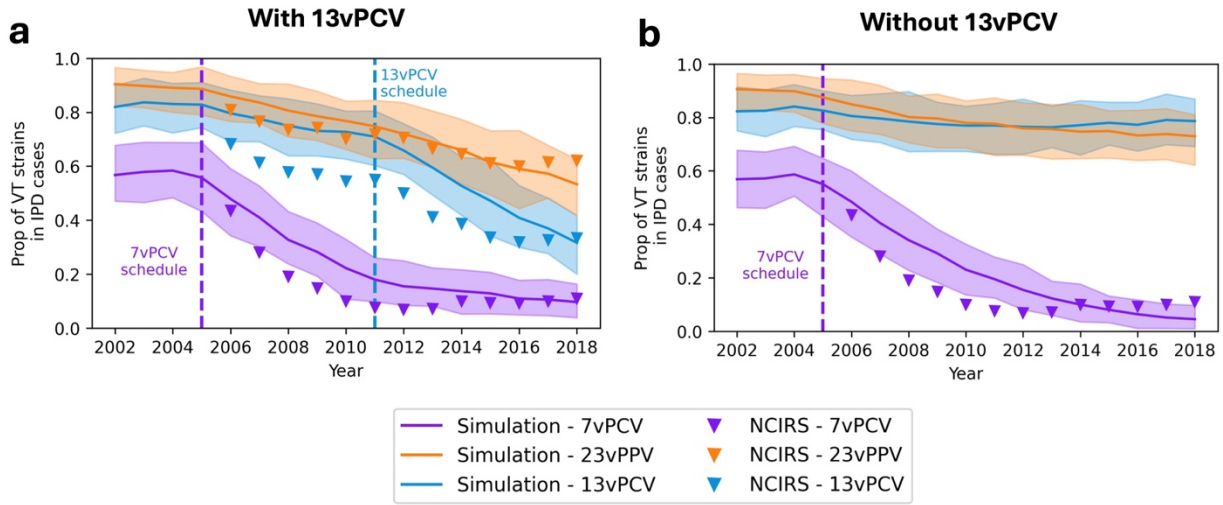

Fig 7: Proportion of vaccine-type serotypes in IPD cases for the period 2002–2018 in (a) Australian vaccination strategy and (b) No 13vPCV scenario. The results represent whole population. 7vPCV is shown in purple while 13vPCV/non 7vPCV and 23vPPV/non 13vPCV are shown in blue and orange, respectively. Mean and 95% quantiles of 100 simulation runs are presented, data is shown as triangles.

With 13vPCV, we observed lower CAP per year, per 100,000 (79.79, 95% CI: [77.53 - 81.85]) and IPD per year, per 100,000 (6.99 95% CI: [6.38 - 7.64]) burden after 2011, respectively, compared to the no 13vPCV scenario (83.96 95% CI: [81.9 – 85.8] and 7.4 95%CI: [6.91 - 7.9], respectively; Fig 8).

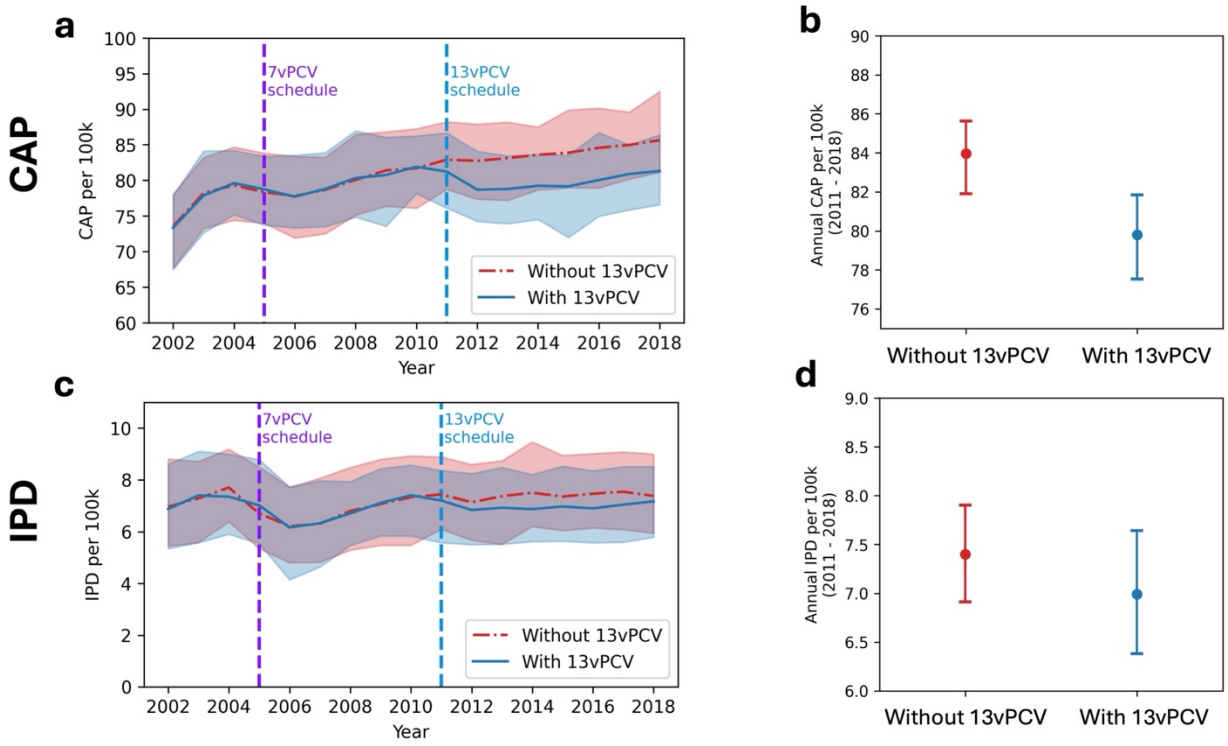

Fig 8: Annual IPD and CAP incidence per year, per 100,000 between 2002—2018. Panels a and b show the annual CAP burden per 100,000 population, and panels c and d show the annual IPD burden per 100,000 population. Panels a and c show the annual disease burden per 100,000 population with and without 13vPCV scenarios. Panels b and d show the average annual disease burden per 100,000 population for the period 2011–2018.

4. Discussion

This paper describes a novel modelling framework that realistically simulates pneumococcal carriage and disease outcome dynamics for evaluation of vaccine strategies. Its development was prompted by the need for a comprehensive model that realistically captures heterogeneities in serotypes, vaccines, and host characteristics to compare efficacy of different vaccine schedules and inform public health decisions for a given population. Our framework has addressed these challenges, enabling modelling of individual serotype transmission in large populations without introducing biases arising from clustered representation of serotypes in carriage and disease. Moreover, the model has sufficient flexibility to be calibrated to diverse populations and to evaluate multiple vaccine formulations and administration scenarios.

Numerous studies have modelled the efficacy of pneumococcal conjugate vaccines, with many utilizing a compartmental modelling approach (*18–20*, *29*). While these models account for the multi-valent nature of *Streptococcus pneumoniae* to some degree, they

often depend on simplifying assumptions about serotype and host representation (*28*). Earlier models tend to use only two serotype groups in relation to the vaccine formulation(s) under study, vaccine-type (VT) and non-vaccine-type (NVT) (*18*, *29*). Recent compartment modelling approaches include more serotype grouping (i.e., seven groupings in Horn et al, 2023 (*38*)). These compartmental models typically assume that an individual can be co-infected by one VT and one NVT serotype, but not by two VT or two NVT serotypes. This assumption has the potential to alter transmission rates once VT serotype circulation decreases following vaccine introduction. Additionally, these models often assume a homogeneous vaccine-induced immune response to vaccine-type serotypes (*18*, *20*, *29*). To account for some variations in immune response, Choi et al. (2019) place one vaccine-type serotype with lower vaccine-induced immunity (ST3) into the NVT compartment, assuming all-or-nothing immune response to vaccine-type serotypes (*20*). In another compartmental modelling work, Choi et al (2024) include only one new vaccine-type compartment to evaluate multiple vaccines which requires recalibrating their model (*39*). Ojal et al (2017) categorize individuals into broad age groups, which makes it challenging to estimate the efficacy of vaccine rollout in different age groups (*40*).

The existing individual-based models (IBMs) tend to model a larger number of serotype groups (ranging from 15-27 (*22–25*)). However, it is important to note that these are generic serotypes, not necessarily reflecting the characteristics of actual serotypes, making their application to decision making about public health interventions challenging. In another IBM, Van Effelterre et al. (2010) focus solely on carriage in infants under 2 years old (*26*). Models that do not cover all age groups cannot estimate the combined efficacy of multiple vaccines, such as those targeting both paediatric and elderly populations.

Using the modelling framework, we captured a realistic impact of vaccine-induced immunity on carriage and disease outcomes. A retrospective analysis of pneumococcal disease trends estimated that the 13vPCV paediatric vaccine schedule in Australia reduced the burdens of CAP and IPD by 5% and 5.5%, respectively. This analysis included relevant local context, including host and pathogen-specific heterogeneities and the adult 23vPPV vaccine programme. The model can be applied to consider likely relative benefits of future pneumococcal vaccine schedules for specific populations without introducing simplifying assumptions (*41*). A key advantage of our approach is that the model can readily incorporate vaccines that do not include all serotypes in existing vaccines.

Our modelling approach also comes with limitations. While incorporating pathogen, host, and vaccine-specific heterogeneities can better capture the realistic dynamics of carriage and disease progression, our model requires more data than existing modelling approaches. However, due to the limited data on carriage available in our setting, we made

simplifying assumptions about the relationship of infection to disease over time and the relative impact of vaccine efficacy against acquisition compared to disease progression. Further analysis of these assumptions is required when more surveillance data on carriage becomes available. In addition, we assumed no natural immunity following an episode of carriage and limited the number of co-infections to two serotypes. Further sensitivity analysis would be needed to understand the impact of these assumptions.

In conclusion, we propose a reliable modelling framework for evaluating vaccine efficacy and informing public health strategies by accurately representing vaccine-induced immunity and simulating the dynamics of serotype transmission and disease progression. While it demands more extensive data than previous models, it offers greater flexibility and accuracy, making it well-suited for assessing various vaccine strategies for specific populations.

Acknowledgements

This work was funded by the Australian Government Department of Health and Ageing National Immunisation Division. We acknowledge expert input to model structure and assumptions by members of the Australian Technical Advisory Group on Immunisation and the National Immunisation Division. We are grateful to Sanjay Jayasinghe and colleagues at the National Centre for Immunisation Research and Surveillance of Vaccine Preventable Diseases (NCIRS) for assistance with data access and interpretation. The manuscript uses publicly available data sourced from the National Notifiable Diseases Surveillance System. Aggregated national level data on admissions related to CAP (source: Australian Institute of Health and Welfare) and infant IPD (source: Enhanced IPD notifications data) were provided through NCIRS for use in this program of work, with approval from the Communicable Disease Enhanced Surveillance System (CDESS). These data may only be accessed with permission from the primary source.

References

1. I. Yildirim, W. P. Hanage, M. Lipsitch, K. M. Shea, A. Stevenson, J. Finkelstein, S. S. Huang, G. M. Lee, K. Kleinman, S. I. Pelton, Serotype specific invasive capacity and persistent reduction in invasive pneumococcal disease. *Vaccine* **29**, 283–288 (2010).

2. W. P. Hausdorff, D. R. Feikin, K. P. Klugman, Epidemiological differences among pneumococcal serotypes. *Lancet Infect Dis* **5**, 83–93 (2005).

3. M. Bertran, J. C. D'Aeth, F. Abdullahi, S. Eletu, N. J. Andrews, M. E. Ramsay, D. J. Litt, S. N. Ladhani, Invasive pneumococcal disease 3 years after introduction of a

reduced 1 + 1 infant 13-valent pneumococcal conjugate vaccine immunisation schedule in England: a prospective national observational surveillance study. *Lancet Infect Dis* **24**, 546–556 (2024).

4. N. J. Andrews, P. A. Waight, P. Burbidge, E. Pearce, L. Roalfe, M. Zancolli, M. Slack, S. N. Ladhani, E. Miller, D. Goldblatt, Serotype-specific effectiveness and correlates of protection for the 13-valent pneumococcal conjugate vaccine: a postlicensure indirect cohort study. *Lancet Infect Dis* **14**, 839–846 (2014).

5. S. Feng, J. McLellan, N. Pidduck, N. Roberts, J. P. Higgins, Y. Choi, A. Izu, M. Jit, S. A. Madhi, K. Mulholland, A. J. Pollard, S. Procter, B. Temple, M. Voysey, Immunogenicity and seroefficacy of pneumococcal conjugate vaccines: a systematic review and network meta-analysis. *Health Technol Assess (Rockv)*, 1–109 (2024).

6. H. Y. Wunrow, R. G. Bender, A. Vongpradith, S. B. Sirota, L. R. Swetschinski, A. Novotney, A. P. Gray, K. S. Ikuta, F. Sharara, E. E. Wool, A. Aali, S. Abd-Elsalam, A. Abdollahi, J. M. Abdul Aziz, H. Abidi, R. G. Aboagye, H. Abolhassani, E. Abu-Gharbieh, L. H. Adamu, T. D. Adane, I. Y. Addo, O. A. Adegboye, T. A. Adekiya, M. Adnan, Q. E. S. Adnani, S. Afzal, S. Aghamiri, Z. B. Aghdam, A. Agodi, B. O. Ahinkorah, A. Ahmad, S. Ahmad, M. Ahmadzade, A. Ahmed, A. Ahmed, J. Q. Ahmed, M. S. Ahmed, K. Akinosoglou, A. Aklilu, M. Akonde, F. Alahdab, T. M. A. AL-Ahdal, F. M. Alanezi, A. H. Albelbeisi, T. B. B. Alemayehu, K. A. Alene, A. Al-Eyadhy, A. A. S. Al-Gheethi, A. Ali, B. A. Ali, L. Ali, S. S. Ali, Y. Alimohamadi, V. Alipour, S. M. Aljunid, S. Almustanyir, R. M. Al-Raddadi, N. Alvis-Guzman, Y. M. Al-Worafi, H. Aly, E. K. Ameyaw, R. Ancuceanu, A. Ansar, G. Ansari, A. E. Anyasodor, J. Arabloo, A. Y. Aravkin, D. Areda, A. A. Artamonov, J. Arulappan, R. T. Aruleba, M. Asaduzzaman, K. A. Atalell, S. S. Athari, D. Atlaw, M. M. W. Atout, S. Attia, T. Awoke, M. K. Ayalew, T. M. Ayana, A. D. Ayele, S. Azadnajafabad, K. Azizian, M. Badar, A. D. Badiye, N. Baghcheghi, M. Bagheri, S. Bagherieh, S. Bahadory, A. A. Baig, A. Barac, S. Barati, M. Bardhan, Z. Basharat, A. Bashiri, B. Basnyat, Q. Bassat, S. Basu, N. S. Bayileyegn, N. Bedi, A. H. Behnoush, A. A. Bekel, M. A. Belete, O. O. Bello, A. S. Bhagavathula, D. Bhandari, P. Bhardwaj, S. Bhaskar, A. N. Bhat, A. Bijani, N. Bineshfar, A. Boloor, S. Bouaoud, D. Buonsenso, K. Burkart, L. A. Cámera, C. A. Castañeda-Orjuela, A. Cernigliaro, J. Charan, V. K. Chattu, P. R. Ching, H. Chopra, S. G. Choudhari, D. J. Christopher, D.-T. Chu, R. A. S. Couto, N. Cruz-Martins, O. Dadras, X. Dai, L. Dandona, R. Dandona, S. Das, N. R. Dash, M. Dashti, F. P. De la Hoz, S. A. Debela, D. Dejen, H. Dejene, D. Demeke, F. M. Demeke, B. H. Demessa, A. K. Demetriades, S. Demissie, D. Dereje, E. Dervišević, H. D. Desai, A. M. Dessie, F. Desta, K. Dhama, S.

Djalalinia, T. C. Do, M. Dodangeh, M. Dodangeh, R.-M. V. Dominguez, D. Dongarwar, H. L. Dsouza, O. C. Durojaiye, A. M. Dziedzic, M. H. Ekat, M. Ekholuenetale, T. C. Ekundayo, M. El Sayed Zaki, H. El-Abid, M. Elhadi, V. G. El-Hajj, W. El-Huneidi, A. A. El-Sakka, H. L. Esayas, A. F. Fagbamigbe, S. Falahi, J. Fares, A. Fatehizadeh, S. A. F. Fatima, N. A. Feasey, G. Fekadu, G. Fetensa, D. Feyissa, F. Fischer, B. Foroutan, P. A. Gaal, M. A. Gadanya, A. Gaipov, B. Ganesan, M. Gebrehiwot, K. G. Gebrekidan, T. G. Gebremeskel, G. M. Gedef, Y. Y. Gela, U. Gerema, B. D. Gessner, M. E. Getachew, K. Ghadiri, K. Ghaffari, S.-H. Ghamari, R. Ghanbari, R. M. M. Ghazy, G. Ghozali, A. B. A. Gizaw, E. V. Glushkova, M. Goldust, M. Golechha, H. A. Guadie, R. A. Guled, M. Gupta, S. Gupta, V. B. Gupta, V. K. Gupta, V. K. Gupta, N. R. Hadi, A. Haj-Mirzaian, S. Haller, S. Hamidi, S. Haque, H. Harapan, A. I. Hasaballah, I. Hasan, H. Hasani, M. Hasanian, H. Hassankhani, M. B. Hassen, K. Hayat, M. Heidari, M. Heidari-Foroozan, R. Heidari-Soureshjani, K. Hezam, R. Holla, N. Horita, M. M. Hossain, M.-S. Hosseini, M. Hosseinzadeh, S. Hostiuc, S. Hussain, N. R. Hussein, S. E. Ibitoye, O. S. Ilesanmi, I. M. Ilic, M. D. Ilic, M. T. Imam, K. C. Iregbu, N. E. Ismail, C. C. D. Iwu, C. Jaja, M. Jakovljevic, E. Jamshidi, A. Javadi Mamaghani, J. Javidnia, M. Jokar, N. Jomehzadeh, N. Joseph, C. E. Joshua, J. J. Jozwiak, Z. Kabir, L. R. Kalankesh, R. Kalhor, V. K. Kamal, H. Kandel, I. M. Karaye, A. Karch, H. Karimi, H. Kaur, N. Kaur, M. Keykhaei, H. Khajuria, A. Khalaji, A. Khan, I. A. Khan, M. Khan, T. Khan, K. Khatab, M. M. Khatatbeh, H. R. Khayat Kashani, J. Khubchandani, M. S. Kim, A. Kisa, S. Kisa, F. Kompani, H. R. Koohestani, N. Kothari, K. Krishan, Y. Krishnamoorthy, M. Kulimbet, M. Kumar, S. D. Kumaran, A. Kuttikkattu, A. Kwarteng, T. Laksono, I. Landires, D. O. Laryea, B. K. Lawal, T. T. T. Le, C. Ledda, S. Lee, S. Lee, G. K. Lema, M. Levi, S. S. Lim, X. Liu, G. Lopes, R. Lutzky Saute, P. H. Machado Teixeira, A. Mahmoodpoor, M. A. Mahmoud, E. Malakan Rad, K. Malhotra, A. A. Malik, B. A. Martinez-Guerra, M. Martorell, V. Mathur, M. Mayeli, J. R. C. Medina, A. Melese, Z. A. Memish, A.-F. A. Mentis, M. A. Merza, T. Mestrovic, I. M. Michalek, L. H. N. Minh, A. Mirahmadi, O. Mirmosayyeb, A. Misganaw, A. K. Misra, J. Moghadasi, N. S. Mohamed, Y. Mohammad, E. Mohammadi, S. Mohammed, M. Mojarrad Sani, H. Mojiri-forushani, A. H. Mokdad, S. Momtazmanesh, L. Monasta, M. A. Moni, E. Mossialos, E. Mostafavi, M. Motaghinejad, A. Mousavi Khaneghah, S. Mubarik, L. Muccioli, J. S. Muhammad, F. Mulita, T. Mulugeta, E. Murillo-Zamora, G. Mustafa, S. Muthupandian, A. J. Nagarajan, F. Nainu, T. S. Nair, S. Nargus, H. Nassereldine, Z. S. Natto, B. P. Nayak, I. Negoi, R. I. Negoi, S. A. Nejadghaderi, H. Q. Nguyen, P. T. Nguyen, V. T. Nguyen, R. K. Niazi, N. Noroozi, H. Nouraei, V. Nuñez-Samudio, K. M. Nuruzzaman, V. E. Nwatah, C. I. Nzoputam, O. J. Nzoputam, B. Oancea, R. M. Obaidur, I. A. Odetokun, R. E. Ogunsakin, O. C. Okonji, A. T. Olagunju, L. T. Olana, I. I. Olufadewa, Y. D. Oluwafemi, K. S. Oumer, A. Ouyahia, M. P A, K. Pakshir, P. N.

Palange, S. Pardhan, R. R. Parikh, J. Patel, U. K. Patel, S. Patil, U. Paudel, S. Pawar, U. Pensato, J. Perdigão, M. Pereira, M. F. P. Peres, I.-R. Petcu, M. Pinheiro, Z. Z. Piracha, N. Pokhrel, M. J. Postma, E. J. S. Prates, I. Qattea, P. R. Raghav, L. Rahbarnia, V. Rahimi-Movaghar, M. Rahman, M. A. Rahman, V. Rahmanian, N. Rahnavard, H. Ramadan, P. Ramasubramani, U. Rani, I. R. Rao, D. Rapaka, Z. A. Ratan, S. Rawaf, E. M. M. Redwan, R. C. Reiner Jr, N. Rezaei, A. Riad, T. M. Ribeiro da Silva, T. Roberts, G. Robles Aguilar, J. A. B. Rodriguez, V. D. Rosenthal, B. Saddik, S. Sadeghian, U. Saeed, A. Safary, F. Saheb Sharif-Askari, N. Saheb Sharif-Askari, A. Sahebkar, M. Sahu, S. A. Sajedi, M. Saki, S. Salahi, S. Salahi, M. A. Saleh, M. Sallam, S. Samadzadeh, A. M. Samy, R. K. Sanjeev, M. Satpathy, A. Seylani, A. Sha'aban, M. Shafie, P. A. Shah, S. Shahrokhi, K. Shahzamani, M. A. Shaikh, S. Sham, M. Shannawaz, A. Sheikh, S. M. Shenoy, P. H. Shetty, J. Il Shin, F. Shokri, S. A. Shorofi, S. Shrestha, M. M. Sibhat, E. E. Siddig, L. M. L. R. Silva, H. Singh, J. A. Singh, P. Singh, S. Singh, R. Sinto, A. A. Skryabina, B. Socea, A. Sokhan, R. Solanki, Y. Solomon, P. Sood, S. Soshnikov, A. Stergachis, M. B. Sufiyan, R. Suliankatchi Abdulkader, A. Sultana, S. S. T Y, E. Taheri, E. Taki, J. J. L. Tamuzi, K.-K. Tan, N. Y. Tat, M.-H. Temsah, D. R. Terefa, P. Thangaraju, N. S. Tibebu, J. H. V. Ticoalu, T. Tillawi, M. B. Tincho, I. I. Tleyjeh, R. Toghroli, M. R. Tovani-Palone, D. G. Tufa, P. Turner, I. Ullah, C. D. Umeokonkwo, B. Unnikrishnan, S. M. Vahabi, A. G. Vaithinathan, R. Valizadeh, S. B. Varthya, T. Vos, Y. Waheed, M. T. Walde, C. Wang, K. G. Weerakoon, N. D. Wickramasinghe, A. S. Winkler, M. Woldemariam, N. A. Worku, C. Wright, D. Y. Yada, S. Yaghoubi, G. A. T. Y. Yahya, C. Y. Y. Yenew, M. Yesiltepe, S. Yi, V. Yiğit, Y. You, H. Yusuf, F. Zakham, M. Zaman, S. Bin Zaman, I. Zare, Z. Zareshahrabadi, A. Zarrintan, M. S. Zastrozhin, H. Zhang, J. Zhang, Z.-J. Zhang, P. Zheng, M. Zoladl, A. Zumla, S. I. Hay, C. J. L. Murray, M. Naghavi, H. H. Kyu, Global, regional, and national burden of meningitis and its aetiologies, 1990–2019: a systematic analysis for the Global Burden of Disease Study 2019. *Lancet Neurol* **22**, 685–711 (2023).

7. B. Wahl, K. L. O'Brien, A. Greenbaum, A. Majumder, L. Liu, Y. Chu, I. Lukšić, H. Nair, D. A. McAllister, H. Campbell, I. Rudan, R. Black, M. D. Knoll, Burden of Streptococcus pneumoniae and Haemophilus influenzae type b disease in children in the era of conjugate vaccines: global, regional, and national estimates for 2000–15. *Lancet Glob Health* **6**, e744–e757 (2018).

8. L. R. Grant, M. P. E. Slack, C. Theilacker, J. Vojicic, S. Dion, R.-R. Reinert, L. Jodar, B. D. Gessner, Distribution of serotypes causing invasive pneumococcal disease in older adults from high-income countries and impact of pediatric and adult vaccination policies. *Vaccine* **41**, 5662–5669 (2023).

9. L. R. Grant, M. P. E. Slack, C. Theilacker, J. Vojicic, S. Dion, R.-R. Reinert, L. Jodar, B. D. Gessner, Distribution of Serotypes Causing Invasive Pneumococcal Disease in Children From High-Income Countries and the Impact of Pediatric Pneumococcal Vaccination. *Clinical Infectious Diseases* **76**, e1062–e1070 (2023).

10. D. M. Musher, R. Anderson, C. Feldman, The remarkable history of pneumococcal vaccination: an ongoing challenge. *Pneumonia* **14**, 5 (2022).

11. K. L. O'Brien, M. C. Steinhoff, K. Edwards, H. Keyserling, M. L. Thoms, D. Madore, Immunologic priming of young children by pneumococcal glycoprotein conjugate, but not polysaccharide, vaccines. *Pediatr Infect Dis J* **15**, 425–30 (1996).

12. R. M. Douglas, H. B. Miles, Vaccination against streptococcus pneumoniae in childhood: Lack of demonstrable benefit in young Australian children. *Journal of Infectious Diseases* **149**, 861–869 (1984).

13. L. R. L. Davies, D. Cizmeci, W. Guo, C. Luedemann, R. Alexander-Parrish, L. Grant, R. Isturiz, C. Theilacker, L. Jodar, B. D. Gessner, G. Alter, Polysaccharide and conjugate vaccines to Streptococcus pneumoniae generate distinct humoral responses. *Sci Transl Med* **14**, 1–13 (2022).

14. S. Moberley, J. Holden, D. P. Tatham, R. M. Andrews, Vaccines for preventing pneumococcal infection in adults. *Cochrane Database of Systematic Reviews* **2013** (2013).

15. K. Feemster, U. K. Buchwald, N. Banniettis, J. G. Joyce, P. Velentgas, T. J. Chapman, I. Yildirim, Immunogenicity of Current and Next-Generation Pneumococcal Conjugate Vaccines in Children: Current Challenges and Upcoming Opportunities. *Open Forum Infect Dis* **11**, 1–9 (2024).

16. K. L. O'Brien, E. V. Millar, E. R. Zell, M. Bronsdon, R. Weatherholtz, R. Reid, J. Becenti, S. Kvamme, C. G. Whitney, M. Santosham, Effect of Pneumococcal Conjugate Vaccine on Nasopharyngeal Colonization among Immunized and Unimmunized Children in a Community-Randomized Trial. *J Infect Dis* **196**, 1211–1220 (2007).

17. A. Melegaro, W. J. Edmunds, Cost-effectiveness analysis of pneumococcal conjugate vaccination in England and Wales. *Vaccine* **22**, 4203–4214 (2004).

18. E. De Cao, A. Melegaro, R. Klok, M. Postma, Optimising Assessments of the Epidemiological Impact in the Netherlands of Paediatric Immunisation with 13-Valent Pneumococcal Conjugate Vaccine Using Dynamic Transmission Modelling. *PLoS One* **9**, e89415 (2014).

19. M. Wasserman, A. Lucas, D. Jones, M. Wilson, B. Hilton, A. Vyse, H. Madhava, A. Brogan, M. Slack, R. Farkouh, Dynamic transmission modelling to address infant pneumococcal conjugate vaccine schedule modifications in the UK. *Epidemiol Infect* **146**, 1797–1806 (2018).

20. Y. H. Choi, N. Andrews, E. Miller, Estimated impact of revising the 13-valent pneumococcal conjugate vaccine schedule from 2+1 to 1+1 in England and Wales: A modelling study. *PLoS Med* **16**, e1002845 (2019).

21. Y. H. Choi, M. Jit, S. Flasche, N. Gay, E. Miller, Mathematical Modelling Long-Term Effects of Replacing Prevnar7 with Prevnar13 on Invasive Pneumococcal Diseases in England and Wales. *PLoS One* **7**, e39927 (2012).

22. S. Flasche, W. John Edmunds, E. Miller, D. Goldblatt, C. Robertson, Y. H. Choi, The impact of specific and non-specific immunity on the ecology of Streptococcus pneumoniae and the implications for vaccination. *Proceedings of the Royal Society B: Biological Sciences* **280** (2013).

23. I. Megiddo, E. Klein, R. Laxminarayan, Potential impact of introducing the pneumococcal conjugate vaccine into national immunisation programmes: an economic-epidemiological analysis using data from India. *BMJ Glob Health* **3**, e000636 (2018).

24. S. Cobey, M. Lipsitch, Niche and Neutral Effects of Acquired Immunity Permit Coexistence of Pneumococcal Serotypes. *Science (1979)* **335**, 1376–1380 (2012).

25. M. Nurhonen, A. C. Cheng, K. Auranen, Pneumococcal Transmission and Disease In Silico: A Microsimulation Model of the Indirect Effects of Vaccination. *PLoS One* **8**, e56079 (2013).

26. T. Van Effelterre, M. R. Moore, F. Fierens, C. G. Whitney, L. White, S. I. Pelton, W. P. Hausdorff, A dynamic model of pneumococcal infection in the United States: Implications for prevention through vaccination. *Vaccine* **28**, 3650–3660 (2010).

27. N. J. Andrews, P. A. Waight, P. Burbidge, E. Pearce, L. Roalfe, M. Zancolli, M. Slack, S. N. Ladhani, E. Miller, D. Goldblatt, Serotype-specific effectiveness and correlates of protection for the 13-valent pneumococcal conjugate vaccine: a postlicensure indirect cohort study. *Lancet Infect Dis* **14**, 839–846 (2014).

28. A. Løchen, R. M. Anderson, Dynamic transmission models and economic evaluations of pneumococcal conjugate vaccines: a quality appraisal and limitations. *Clinical Microbiology and Infection* **26**, 60–70 (2020).

29. A. Melegaro, Y. H. Choi, R. George, W. J. Edmunds, E. Miller, N. J. Gay, Dynamic models of pneumococcal carriage and the impact of the Heptavalent Pneumococcal Conjugate Vaccine on invasive pneumococcal disease. *BMC Infect Dis* **10**, 90 (2010).

30. Y. H. Choi, M. Jit, N. Gay, N. Andrews, P. A. Waight, A. Melegaro, R. George, E. Miller, 7-Valent Pneumococcal Conjugate Vaccination in England and Wales: Is It Still Beneficial Despite High Levels of Serotype Replacement? *PLoS One* **6**, e26190 (2011).

31. Australian Bureau of Statistics, Population. https://www.abs.gov.au/statistics/people/population.

32. Macro Trends, Australia Population Growth Rate 1950-2024. https://www.macrotrends.net/global-metrics/countries/aus/australia/population.

33. K. Prem, A. R. Cook, M. Jit, Projecting social contact matrices in 152 countries using contact surveys and demographic data. *PLoS Comput Biol* **13**, e1005697 (2017).

34. A. Kabir, A. T. Newall, D. Randall, R. Menzies, S. Sheridan, S. Jayasinghe, P. Fathima, B. Liu, H. Moore, P. McIntyre, H. F. Gidding, Estimating pneumococcal vaccine coverage among Australian Indigenous children and children with medically at-risk conditions using record linkage. *Vaccine* **39**, 1727–1735 (2021).

35. O. Frank, C. De Oliveira Bernardo, D. A. González-Chica, K. Macartney, R. Menzies, N. Stocks, Pneumococcal vaccination uptake among patients aged 65 years or over in Australian general practice. *Hum Vaccin Immunother* **16**, 965–971 (2020).

36. National Notifiable Diseases Surveillance System, National Notifiable Diseases Surveillance System (NNDSS) public dataset – pneumococcal disease (invasive) (2024). https://www.health.gov.au/resources/publications/national-notifiable-diseases-surveillance-system-nndss-public-dataset-pneumococcal-disease-invasive?language=en.

37. E. M. Dunne, K. Carville, T. V. Riley, J. Bowman, A. J. Leach, A. W. Cripps, D. Murphy, P. Jacoby, D. Lehmann, Aboriginal and non-Aboriginal children in Western Australia carry different serotypes of pneumococci with different antimicrobial susceptibility profiles. *Pneumonia* **8**, 15 (2016).

38. M. Horn, C. Theilacker, R. Sprenger, C. von Eiff, E. Mahar, J. Schiffner-Rohe, M. W. Pletz, M. van der Linden, M. Scholz, Mathematical modeling of pneumococcal transmission dynamics in response to PCV13 infant vaccination in Germany predicts

increasing IPD burden due to serotypes included in next-generation PCVs. *PLoS One* **18**, 1–23 (2023).

39. Y. H. Choi, M. Bertran, D. J. Litt, S. N. Ladhani, E. Miller, Potential impact of replacing the 13-valent pneumococcal conjugate vaccine with 15-valent or 20-valent pneumococcal conjugate vaccine in the 1 + 1 infant schedule in England: a modelling study. *Lancet Public Health* **9**, e654–e663 (2024).

40. J. Ojal, S. Flasche, L. L. Hammitt, D. Akech, M. C. Kiti, T. Kamau, I. Adetifa, M. Nurhonen, J. A. G. Scott, K. Auranen, Sustained reduction in vaccine-type invasive pneumococcal disease despite waning effects of a catch-up campaign in Kilifi, Kenya: A mathematical model based on pre-vaccination data. *Vaccine* **35**, 4561–4568 (2017).

41. P. De Wals, New-generation pneumococcal vaccines for children. *Lancet Public Health* **9**, e638–e639 (2024).